Swarm and Evolutionary Computation 27 (2016) 169–179

Contents lists available at ScienceDirect

Swarm and Evolutionary Computation

journal homepage: www.elsevier.com/locate/swevo

Regular Paper

Coordinated design of power system stabilizers and TCSC employing improved harmony search algorithm

G. Naresh [a,*], M. Ramalinga Raju [b], S.V.L. Narasimham [c]

[a] Department of EEE, Pragati Engineering College, Surampalem, Andhra Pradesh, India
[b] Department of EEE, University College of Engineering Kakinada, JNTUK, Kakinada, Andhra Pradesh, India
[c] Department of CSE, School of Information Technology, JNTUH, Hyderabad, Andhra Pradesh, India

ARTICLE INFO

Article history:
Received 21 May 2014
Received in revised form
20 October 2015
Accepted 25 November 2015
Available online 4 December 2015

KeyWords:
Damping
Improved Harmony Search Algorithm
Power System Stabilizers
TCSC

ABSTRACT

Power System Stabilizers (PSS) are generally employed to damp electromechanical oscillations by providing auxiliary stabilizing signals to the excitation system of the generators. But it has been found that these Conventional PSS (CPSS) do not provide sufficient damping for inter-area oscillations in multi-machine power systems. Thyristor Controlled Series Capacitor (TCSC) has immense potential in damping of inter-area power swings and in mitigating the sub-synchronous resonance. In this paper Improved Harmony Search Algorithm (IHSA) has been proposed for coordinated design of multiple PSS and TCSC in order to effectively damp the oscillations. The results obtained by using IHSA on WSCC 3-machine, 9-bus system are found to be superior compared to the results obtained using Bacterial Swarm Optimization (BSO) algorithm. The damping performance of conventional PSS and TCSC controllers is also compared with coordinated design of IHSA based PSS and TCSC on New England 10-machine, 39-bus system over wide range of operating conditions and contingencies. To demonstrate the effectiveness of the proposed technique the results obtained on this test system are also compared with the results obtained with Genetic Algorithm (GA), Particle Swarm Optimization (PSO), Harmony Search Algorithm (HSA) and Bacterial Swarm Optimization (BSO).

1. Introduction

Power systems are complex nonlinear systems and often exhibit low frequency power oscillations due to insufficient damping. These oscillations may sustain and increase, thus causing the separation of system if no adequate damping is available [1]. Conventional Power System Stabilizers (CPSS) are widely used to suppress the generator electromechanical oscillations and enhance the overall stability of power systems. CPSS based on linear control theory can very well be tuned to an operating condition and will provide excellent damping over a certain range around the design point. However, CPSS parameters may not be optimal for whole set of possible system parameters, operating conditions and configurations.

A comprehensive analysis of the effects of the different CPSS parameters on the overall dynamic performance of the power system has been presented in [2]. It is shown that the appropriate selection of CPSS parameters results in satisfactory performance during system upsets. Robust design of CPSS in multi-machine power systems using global optimization technique like genetic algorithm (GA) [3,4], and other heuristic techniques like tabu search (TS) [5], simulated annealing (SA) [6], particle swarm optimization (PSO) [7–9], bacterial foraging (BF) [10] and harmony search (HS) [11] have attracted the attention in the field of PSS parameter optimization. However, these techniques might fail by getting trapped in one of the local optimal.

Although PSSs provide supplementary feedback stabilizing signals, these controllers may not produce adequate damping during some operating conditions, and other effective controllers which can work in coordination with PSS are needed. Advancements in power electronic technologies have made the application of Flexible AC Transmission Systems (FACTS) devices to alleviate such conditions by controlling the power flow along the transmission lines which improves power oscillations damping [12]. Among these FACTS devices, the Thyristor Controlled Series Capacitor (TCSC) is a multi-functional FACTS controller, which allows quick and continuous changes of the transmission line impedance. TCSC has immense potential and application in precisely regulating the power flow on a transmission line, mitigating the sub-synchronous resonance, improving the transient stability and damping inter-area power swings [13].

* Corresponding author at: Electrical and Electronics Engineering at Pragati Engineering College, Surampalem, East Godavari District, Andhra Pradesh 533437, India. Mobile no.: +91 9849898440.
E-mail address: naresh.elec@gmail.com (G. Naresh).

http://dx.doi.org/10.1016/j.swevo.2015.11.003
2210-6502/

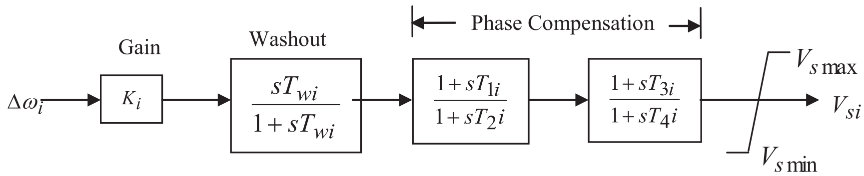

Fig. 1. Structure of PSS.

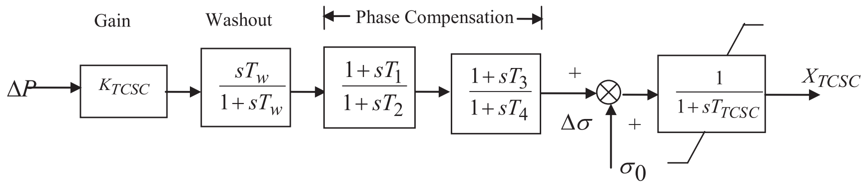

Fig. 2. Structure of TCSC controller.

The applications of TCSC for power oscillation damping and stability enhancement can be found in [14–16]. However, these works are limited for single machine connected to infinite bus (SMIB) system. A reduced rule base self-tuning fuzzy PI controller (STFPIC) for TCSC is proposed in [17]. A supplementary damping control system design for TCSC based on natural inspired Virtual Bees Algorithm (VBA) is presented in [18]. An attempt is made to suppress oscillations in a multi-machine power system using bacterial foraging algorithm based TCSC is illustrated in [19].

In recent years, little work has been reported in the literature on the coordination problem investigation of multiple damping controllers for multi-machine power systems [20–22]. However, uncoordinated local control of TCSC controller and PSS may cause unwanted interactions that may further result in system destabilization. To improve overall system performance, many studies were made on the coordination among PSS and FACTS controllers [23–25]. Unfortunately, the problem of coordinated design of conventional power oscillation damping controllers is a multimodal optimization problem and conventional tuning methods may not provide sufficient damping for stabilizing inter-area oscillations. Hence the meta-heuristic methods, which are widely used for global optimization problems, have been used to solve this coordinated design problem. Abido et al. [26] have presented coordinated design of a PSS and an SVC-based controller using real coded Genetic Algorithm (GA). Particle Swarm Optimization (PSO) for simultaneous coordination designing of PSS and TCSC damping controller in multi-machine power system is developed in [27]. But GA exhibits degraded efficiency when the system has a highly *epistatic* objective function (i.e., where the parameters being optimized are highly correlated) and number of parameters to be optimized are large [28]. PSO suffers from the partial optimism, which causes the less exact at the regulation of its speed and the direction. Further, PSO algorithm cannot solve the problems of scattering and non-coordinate system optimization [29].

Several optimization techniques using the swarming principle have been adopted to solve a variety of engineering problems in the recent past. An improved multi-objective particle swarm optimization algorithm is applied for improving power system stability and to economic load dispatch problem in [30,31]. Ali et al. [32] have proposed a novel bacterial swarm optimization algorithm for simultaneous design of PSS and TCSC. A novel approach for determining the optimal solution of economic dispatch (ED) problem employing Firefly Algorithm (FA) and hybrid of bacterial foraging and simplified swarm optimization algorithm are presented in [33,34]. Ghasemi et al. [35,36] have adopted modified teaching learning algorithm, double differential evolution algorithm and hybrid modified imperialist competitive algorithm–invasive weed optimization (IWO) for optimal reactive power dispatch problem. In [37,38] modified imperialist competitive algorithm and hybrid of imperialist competitive algorithm and teaching learning algorithm have been applied for optimal power flow problem.

In this paper, Improved Harmony Search Algorithm (IHSA) is employed for coordinated design of the parameters of PSS and TCSC controllers simultaneously. By minimizing the objective function in which the influences of both PSS and TCSC controllers are considered simultaneously, interactions among these controllers are improved. These controllers have been applied and tested on New England 10-machine, 39-bus system under wide range of loading conditions and severe disturbances. The eigenvalue analysis and non-linear simulation results are presented to demonstrate the effectiveness and robustness of the proposed controllers in damping low frequency inter-area oscillations.

2. Statement of the problem

2.1. Power system model

A power system can be modeled by a set of nonlinear differential equations as $\dot{X} = f(X, U)$, where X is the vector of the state variables, and U is the vector of input variables. In this study, all the generators in the power system are represented by their fifth order models and equipped with single time constant fast exciters.

For a given operating condition, the multi-machine power system is linearized around the operating point. The closed loop eigenvalues of the system are computed and the desired objective function is formulated using only the unstable or lightly damped electromechanical eigenvalues, keeping the constraints of all the system modes stable under any condition.

2.2. PSS structure

The structure of the speed based conventional PSS considered in this study is shown in Fig.1.

Here $\Delta\omega_i$ is the deviation of the speed of the rotor of ith generator from synchronous speed. The $\frac{sT_{wi}}{1+sT_{wi}}$ term in the above diagram is the washout term with a time constant T_{wi} which is generally 1–20 s. The washout block serves as a high-pass filter to allow signals in the range of 0.2–2.0 Hz associated with rotor oscillations. T_{wi} is chosen such that undesirable generator voltage excursions during system-islanding are eliminated. The phase compensation block provides compensation for the phase lag/lead that is introduced in the circuit between the exciter input (i.e. PSS

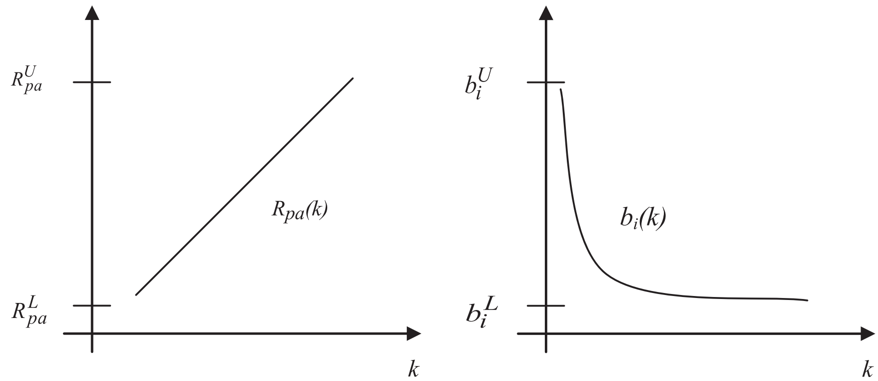

Fig. 3. Variation of R_{pa} and b_i with increase in iteration number.

output) and the electrical torque. In this study $T_w = 10$ s and the parameters to be optimized are $\{K_i, T_{1i}, T_{2i};\ i = 1,2\ 3,\ldots,m,$ where m is the number of generators$\}$, assuming $T_{1i} = T_{3i}$ and $T_{2i} = T_{4i}$.

2.3. TCSC structure

Here K_{TCSC} is TCSC gain and T_w is washout time constant. In this study, $T_w = 10$ s and $T_1 = T_3$ and $T_2 = T_4$ are used. The structure of the TCSC based damping controller is shown in Fig. 2. This controller may be considered as a lead lag compensator. It comprises gain block, signal washout block and a two stage lead-lag compensator. Many input signals have been proposed for the FACTS to damp the system oscillations. Since FACTS controllers are located in the transmission systems, local input signals are always preferred. Transmission line active power has been proposed as an effective input signal for the design of series FACTS Controller [27,39]. For this reason, active power of the transmission line is selected as the input signal in this paper.

2.4. Objective function

In this paper, a comprehensive assessment of the effects of coordinated application of PSS and TCSC damping controllers has been carried out. A multi-objective problem is formulated to optimize a composite set of two eigenvalue-based objective functions comprising the desired damping factor and damping ratio of the lightly damped and undamped electromechanical modes. The use of the first objective function will result in PSS that shift the lightly damped and undamped electromechanical modes to the left-hand side of a vertical line in the complex s-plane, resulting in improved damping factor. The use of the second objective function will yield PSS and TCSC settings that place these modes in a wedge-shape sector in the complex s-plane, thus improving the damping ratio of these modes. Consequently, the use of the multi-objective function guarantees the improvement of relative stability and minimization of peak overshoot.

The parameters of PSS and TCSC are tuned simultaneously so as to minimize the following objective function:

$$J = J1 + \alpha \cdot J2 \tag{1}$$

where

$$J1 = \sum_{j=1}^{NP} \sum_{\sigma_{i,j} \geq \sigma_0} [\sigma_0 - \sigma_{i,j}]^2 \tag{2}$$

$$J2 = \sum_{j=1}^{NP} \sum_{\xi_{i,j} \geq \xi_0} [\xi_0 - \xi_{i,j}]^2 \tag{3}$$

and α is a positive constant

Here $\sigma_{i,j}$ is the real part and $\xi_{i,j}$ is the damping ratio of ith eigenvalue of jth operating point, subject to the constraints that finite bounds are placed on the power system stabilizer parameters.

It is necessary to mention here that only the unstable or lightly damped electromechanical modes of oscillations are relocated. The design problem can be formulated as the following constrained optimization problem, where the constraints are the PSS parameter bounds:

Minimize J subject to

$$\begin{aligned} &K_{i_{min}} \leq K_i \leq K_{i_{max}} \\ &T_{1i_{min}} \leq T_{1i} \leq T_{1i_{max}} \\ &T_{2i_{min}} \leq T_{2i} \leq T_{2i_{max}} \\ &K_{TCSC_{min}} \leq K_{TCSC} \leq K_{TCSC_{max}} \\ &T_{1_{min}} \leq T_1 \leq T_{1_{max}} \\ &T_{2_{min}} \leq T_2 \leq T_{2_{max}} \end{aligned} \tag{4}$$

In this study, σ_0 and ξ_0 are chosen to be -2.0% and 20% respectively. Several values for weight α are tested and it is observed that effect of α on final goal is minimal. Here α is taken as 10 [4]. Typical ranges of the optimized parameters for PSS are [0.01, 50] for K_i and [0.01, 1.0] for T_{1i} and T_{2i}. TCSC bounds are [0.01, 100] for K_{TCSC} and [0.01, 1.0] for T_1 and T_3.

3. Improved Harmony Search Algorithm

The Harmony Search Algorithm is a phenomenon-mimicking, music inspired new meta heuristic algorithm proposed by Geem [40]. It was inspired by the improvisation process of the musicians who collectively play their musical instruments (population members) to come out with a pleasing harmony (global optimum solution). The HSA is simple in concept, less in parameters and easy in implementation. It is inspired by the improvisation process of the musicians who collectively play their musical instruments to come out with a pleasing harmony. The perfectly pleasing harmony is determined by the audio esthetic standard. Compared with other heuristic algorithms, optimal balance of diversification and intensification, which are also referred as exploration and exploitation to achieve global optimum solution, is achieved in HSA [41]. In addition, the implementation of HS algorithm is also easier. The important property of HSA is that it is less sensitive to the chosen parameters, i.e., there is no need to fine-tune these parameters to get quality solutions.This algorithm has been successfully applied to a variety of optimization problems like traveling salesperson problem, tour routing, music composition, water network design, structural design etc. The main steps of Harmony Search Algorithm are as follows:

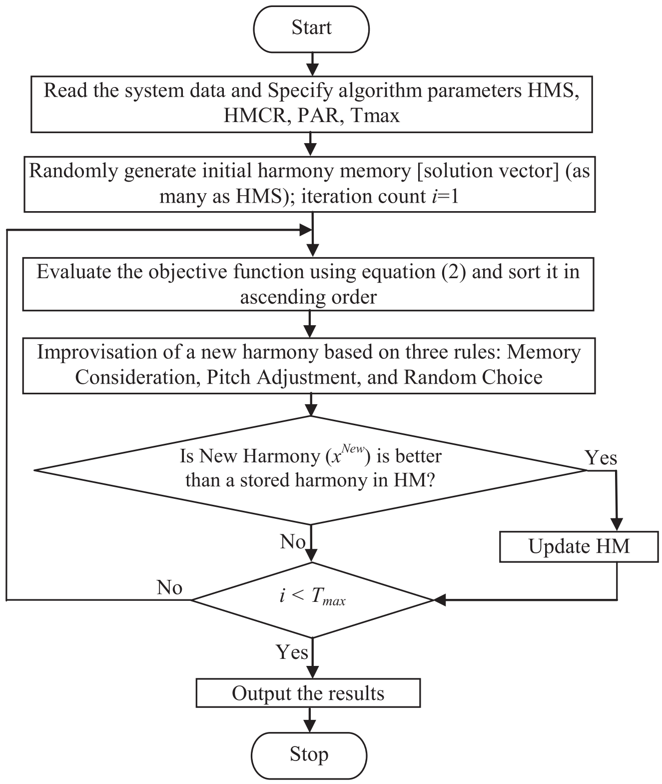

Fig. 4. Flowchart of Improved Harmony Search Algorithm.

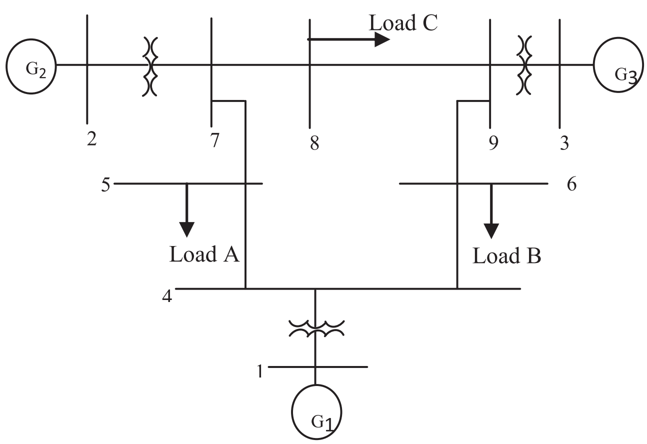

Fig. 5. WSCC 3-machine, 9-bus system.

Table 1
Loadings and generations in PU on system 100-MVA base.

Load	Light Load		Normal Load		Heavy Load	
	P	*Q*	*P*	*Q*	*P*	*Q*
A	0.70	0.350	1.25	0.5	2.00	0.90
B	0.50	0.300	0.90	0.30	1.80	0.60
C	0.60	0.200	1.00	0.35	1.60	0.65
Local load at G1	0.60	0.200	1.00	0.35	1.60	0.65
Gen#						
G1	0.9649	0.2230	1.7164	0.6205	3.5730	1.8143
G2	1.0000	−0.1933	1.6300	0.0665	2.2000	0.7127
G3	0.4500	−0.2668	0.8500	−0.1086	1.3500	0.4313

1. Initialize the optimization problem and algorithm parameters.
2. Initialize the Harmony memory.
3. Improve a new harmony.
4. Update the new harmony.
5. Check for termination condition.

Step 1: *Initialization the optimization problem and algorithm parameters*

i) *Optimization problem*
The general optimization problem is specified as follows:
Minimize/maximize $f(x)$
Subject to $x_i \in X\ i = 1, 2....N$
where f(x) is the optimization function, x is the set of each decision variable x_i, N is the number of decision variables and X_i is the set of possible range of values for each decision variable such that

$$X_i^L \le X_i \le X_i^U \tag{5}$$

where $X_i{}^L$ and $X_i{}^U$ are the lower and upper bounds of the each decision variable.

ii) *Algorithm parameters*
HSA parameters that are to be specified are Harmony Memory Size (HMS), Harmony Memory Considering Rate (HMCR), Pitch Adjusting Rate (R_{pa}) and band width (b_i). The Harmony Memory (HM) is a memory location where all the solution vectors are stored. Here HMCR, R_{pa} and b_i are used to improve the solution vector.

Step 2: Initialize Harmony Memory

In this step, the HM matrix is filled with as many randomly generated solution vectors as the HMS

The elements in the HM are determined with randomly generated solution vectors. For instance the *i*th variable x_i can be generated as

$$x_i = x_i^L + rand(1) * (x_i^U - x_i^L) \tag{6}$$

where and $X_i{}^U$ are the lower and upper bounds of the each decision variable.

Step 3: Improvise a New Harmony:

A new Harmony vector $\bar{x} = \left(x_1', x_2', \ldots, x_N'\right)$ is generated based on three criteria

(1) Memory consideration
(2) Pitch adjustment
(3) Random selection

For instance the *i*th variable x_i' is chosen from the historical values stored in the HM (hence called memory consideration) with a probability of HMCR, and (1-HMCR) is the rate of random selection: for example an HMCR of 0.7 depicts that HSA will choose the decision variable value from historically stored values in HM with a probability of 70% or from the entire possible range with a probability of 30%. Further every component obtained by memory consideration is pitch adjusted with a Pitch Adjusting Rate of R_{pa}. If pitch adjustment is enforced x_i' is replaced with

$$x_i' = x_i^{(j)} + rand(1) * b_i \tag{7}$$

where b_i is the distance bandwidth of the *i*th variable in the new vector.

R_{pa} and b_i in HS algorithm are very important parameters in fine-tuning of optimized solution vectors, and can be potentially useful in adjusting convergence rate of algorithm to optimal solution. So fine adjustment of these parameters are of great interest. Small R_{pa} values with large b_i values can cause to poor performance of the algorithm and considerable increase in iterations needed to

Table 2
Tuned parameters of coordinated controllers using BSO and IHSA.

Gen#	Tuned parameters using BSO [9]			Tuned parameters using IHSA		
	K	T_1	T_2	K	T_1	T_2
G1	23.0006	0.3282	0.0754	19.4986	0.6198	0.4638
G2	16.3196	0.1945	0.5846	2.3682	0.8892	0.1904
G3	3.8619	0.1177	0.7399	3.4267	0.6568	0.3882
TCSC	1.0958	0.8704	0.1741	6.7284	0.7688	0.3294

Table 3
Comparison of eigenvalues and damping ratios for different loadings.

	Light load	Normal load	Heavy load
Without controller	−10.60 ± 11.48i, 0.6782 − **0.95** ± 8.61i **0.1103**	−11.17 ± 10.43i, 0.7307 − **0.34** ± 8.81i, **0.0386**	−11.35 ± 11.28i, 0.7093 − **0.15** ± 9.00i, **0.0167**
BSOPSS + BSOTCSC [9]	−4.51 ± 7.38i, **0.5215** − **1.09** ± 0.71i, 0.8379	−4.15 ± 8.15i, **0.4538** − **1.04** ± 0.84i, 0.7779	−4.49 ± 7.77i, **0.5003** − **1.03** ± 0.86i, 0.7676
IHSAPSS + IHSATCSC	−9.63 ± 8.12i 0.7646 − **3.16** ± **4.10i 0.6114**	−10.57 ± 5.60i 0.88 − **2.78** ± **4.09i 0.56**	−10.75 ± 5.58i, 0.8876 − **2.59** ± **4.09i, 0.5335**

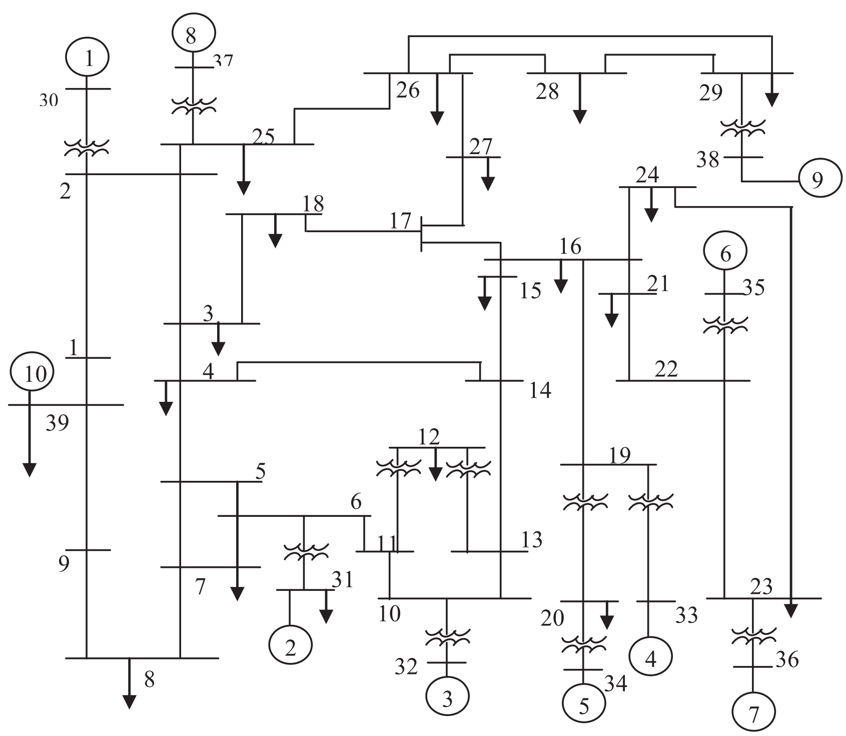

Fig. 6. New England 10-machine, 39-bus system.

Table 4
Residues obtained using $\Delta P/\Delta K_c$.

line 26–29	9.016
line 26–28	4.662
line 28–29	4.086
line 16–17	2.924
line 16–19	2.014
line 17–27	1.396
line 2–3	1.090
line 25–26	0.730
line 23–24	0.614
line 16–21	0.490
line 4–14	0.122
line 5–6	0.008
line 15–16	0.0003

Table 5
Operating scenarios.

Scenario	Description
Scenario 1	All lines in service
Scenario 2	Outage of line connecting bus no. 14 and 15
Scenario 3	Outage of line connecting bus no. 21 and 22
Scenario 4	Increase in generation of G7 by 25% and loads at buses 16 and 21 by 25%, with the outage of line 21–22

find optimum solution. Although small b_i values in final generations increase the fine-tuning of solution vectors, but in early generations b_i must take a bigger value to enforce the algorithm to increase the diversity of solution vectors. Furthermore large R_{pa} values with small b_i values usually cause the improvement of best solutions in final generations which algorithm converged to optimal solution vector. These observations lead to the development of Improved Harmony Search Algorithm [42].

The key difference between Improved Harmony Search Algorithm (IHSA) and traditional HSA is in the way of adjusting R_{pa} and b_i. The traditional HSA algorithm uses fixed value for both R_{pa} and

Table 6
Tuned parameters of damping controllers.

Location	Controller	Individual Design IHSA			Coordinated Design IHSA		
		K	T_1	T_2	K	T_1	T_2
G1	PSS	38.1335	0.5002	0.1176	36.9362	0.5443	0.1541
G2	PSS	14.9866	0.5506	0.0670	15.2106	0.5726	0.1665
G3	PSS	11.8254	0.5604	0.1499	10.4251	0.6381	0.1174
G4	PSS	1.7998	0.5701	0.0482	1.8021	0.7353	0.1058
G5	PSS	17.9988	0.5514	0.0744	18.4951	0.5492	0.2611
G6	PSS	11.9225	0.5273	0.1543	12.0529	0.6656	0.1785
G7	PSS	5.1818	0.5176	0.0813	5.2918	0.6465	0.1136
G8	PSS	4.2996	0.5283	0.0781	4.3015	0.8002	0.0982
G9	PSS	14.9888	0.5427	0.1585	15.0818	0.5944	0.1405
G10	PSS	49.8668	0.5678	0.0724	49.9886	0.7381	0.1274
26–29	TCSC	45.84	0.7863	0.3895	48.82	0.5824	0.2357

Table 7
Comparison of eigenvalues and damping ratios for different scenarios.

	No controller	IHSATCSC	IHSAPSS	IHSAPSS + IHSATCSC
Scenario 1	−1.1878 ± 10.6655i, 0.1107	−1.7874 ± 12.5751i, 0.1407	−2.8599 ± 12.8151i, 0.2178	−2.3661 ± 11.4315i, 0.2027
	−0.3646 ± 8.8216i, 0.0413	−1.3322 ± 11.2722i, 0.1174	−2.4046 ± 11.3734i, 0.2069	−2.0343 ± 10.6661i, **0.1874**
	−0.3063 ± 8.5938i, 0.0356	−1.8386 ± 11.1594i, 0.1626	−2.0207 ± 10.6026i, **0.1872**	−2.3746 ± 8.9921i, 0.2553
	−0.2718 ± 8.1709i, 0.0332	−1.1093 ± 9.1192i, 0.1208	−2.2684 ± 8.9997i, 0.2444	**−1.9439 ± 8.7168i,** 0.2177
	−0.0625 ± 7.2968i, 0.0086	−0.5143 ± 8.5043i, 0.0604	−1.9961 ± 8.5929i, 0.2263	−3.7288 ± 6.0353i, 0.5256
	−0.1060 ± 6.8725i, 0.0154	−1.1463 ± 7.5156i, 0.1508	−3.7091 ± 6.2721i, 0.5090	−2.9649 ± 4.5378i, 0.5470
	0.2579 ± 6.1069i, −0.0422	−0.1590 ± 7.3838i, 0.0215	−2.9722 ± 4.5233i, 0.5491	−2.1137 ± 3.6619i, 0.4999
	0.0620 ± 6.1767i, −0.0100	**−0.1037 ± 6.4182i, 0.0162**	−2.0277 ± 3.7264i, 0.4780	−2.5393 ± 3.4123i, 0.5970
	0.0794 ± 3.9665i, −0.0200	−1.2991 ± 4.8171i, 0.2604	**−1.9395 ± 3.2066i,** 0.5175	−2.0725 ± 3.3061i, 0.5311
Scenario 2	−1.1888 ± 10.6603i, 0.1108	−1.7880 ± 12.5610i, 0.1409	−2.8550 ± 12.8177i, 0.2174	−2.0493 ± 10.6651i, **0.1887**
	−0.3642 ± 8.8221i, 0.0412	−1.3352 ± 11.2674i, 0.1177	−2.4645 ± 11.3444i, 0.2123	−3.5043 ± 9.8431i, 0.3354
	−0.3087 ± 8.5753i, 0.0360	−1.8404 ± 11.1650i, 0.1626	−2.1092 ± 10.4931i, 0.1971	−2.2356 ± 9.7855i, 0.2227
	−0.2727 ± 8.1706i, 0.0334	−1.0769 ± 9.1107i, 0.1174	**−1.6957 ± 8.9980i, 0.1852**	**−1.7076 ± ± 8.3194i,** 0.2011
	−0.0643 ± 7.2859i, 0.0088	−0.4993 ± 8.4895i, 0.0587	−2.9908 ± 8.3811i, 0.3361	−3.6894 ± 6.0566i, 0.5202
	−0.1000 ± 6.7243i, 0.0149	−0.1624 ± 7.3781i, **0.0220**	−3.7275 ± 6.2599i, 0.5116	−2.6117 ± 4.3178i, 0.5176
	0.2997 ± 6.1030i, −0.0490	−1.6768 ± 6.7869i, 0.2399	−2.6972 ± 4.1651i, 0.5436	−2.9883 ± 3.5750i, 0.6413
	0.0824 ± 5.7423i, −0.0143	**−0.1528 ± 6.0554i,** 0.0252	−2.1317 ± 3.6879i, 0.5004	−1.8910 ± 3.7298i, 0.4522
	0.0844 ± 3.8066i, −0.0222	−1.2664 ± 5.8716i, 0.2108	−1.9063 ± 3.2291i, 0.5084	−1.9519 ± 3.2304i, 0.5171
Scenario 3	−1.1686 ± 10.6268i, 0.1093	−1.7257 ± 11.9617i, 0.1428	−2.6619 ± 12.7107i, 0.2050	−2.6235 ± 12.6693i, 0.2028
	−0.3413 ± 8.7548i, 0.0390	−1.3222 ± 11.2307i, 0.1169	−2.0211 ± 10.6048i, 0.1872	−3.7998 ± 10.1122i, 0.3518
	−0.3013 ± 8.4738i, 0.0355	−1.8623 ± 11.0809i, 0.1657	−4.1687 ± 9.4233i, 0.4046	−2.0342 ± 10.6655i, **0.1874**
	−0.2575 ± 8.0464i, 0.0320	−0.5383 ± 8.4666i, 0.0635	−1.8179 ± 9.6012i, **0.1860**	−1.8456 ± 9.6184i, 0.1884
	−0.0615 ± 7.3143i, 0.0084	−0.8024 ± 8.2285i, 0.0971	**−1.7205 ± 8.0498i,** 0.2090	**−1.8292 ± 8.0582i,** 0.2214
	0.1283 ± 6.1862i, −0.0207	−0.1574 ± 7.4050i, 0.0212	−3.6748 ± 6.3246i, 0.5024	−3.6881 ± 6.0703i, 0.5192
	0.0427 ± 6.0556i, −0.0070	**−0.0980 ± 6.3997i, 0.0153**	−2.4239 ± 4.2576i, 0.4948	−2.5788 ± 4.3477i, 0.5102
	0.2018 ± 5.8565i, −0.0344	−1.1680 ± 5.7492i, 0.1991	−1.7665 ± 3.8262i, 0.4192	−1.8696 ± 3.7245i, 0.4486
	0.1659 ± 3.7438i, −0.0443	−1.0378 ± 3.3251i, 0.2979	−1.8474 ± 3.2106i, 0.4987	−1.9653 ± 3.2309i, 0.5197
Scenario 4	−1.1645 ± 10.6163i, 0.1090	−1.6579 ± 11.9805i, 0.1371	−2.7941 ± 12.8369i, 0.2127	−2.7947 ± 12.7309i, 0.2144
	−0.3256 ± 8.8902i, 0.0366	−1.3152 ± 11.2088i, 0.1165	−2.0100 ± 10.6302i, 0.1858	−3.7330 ± 10.3166i, 0.3403
	−0.2977 ± 8.4483i, 0.0352	−1.8702 ± 11.0437i, 0.1670	−4.2383 ± 9.5219i, 0.4066	−2.0218 ± 10.6883i, 0.1859
	−0.2587 ± 8.0346i, 0.0322	−0.5382 ± 8.4526i, 0.0635	−1.6874 ± 9.5704i, **0.1736**	**−1.7136 ± 9.6083i, 0.1756**
	−0.0575 ± 7.3333i, 0.0078	−0.7473 ± 8.1568i, 0.0912	−1.6785 ± 7.9162i, 0.2074	−1.7885 ± 7.9247i, 0.2202
	0.1557 ± 6.1630i, −0.0253	−0.1533 ± 7.4245i, 0.0206	−3.6719 ± 6.3395i, 0.5012	−3.6869 ± 6.0807i, 0.5185
	0.0586 ± 6.0959i, −0.0096	**−0.0933 ± 6.3887i, 0.0146**	−2.3565 ± 4.1807i, 0.4910	−2.5093 ± 4.3073i, 0.5034
	0.2089 ± 5.6778i, −0.0368	−0.8687 ± 5.7477i, 0.1494	**−1.6237 ± 3.8188i,** 0.3913	−1.7991 ± 3.7173i, 0.4356
	0.2352 ± 3.6446i, −0.0644	−0.8239 ± 3.2401i, 0.2464	−1.8200 ± 3.2130i, 0.4929	−1.9405 ± 3.2146i, 0.5168

b_i. The main drawback of HSA appears in the number of iterations the algorithm needs to find an optimal solution. To improve the performance of the HSA and eliminate the drawbacks lies with fixed values of R_{pa} and b_i, IHSA uses variable R_{pa} and b_i in improvisation step (Step 3). The variation of R_{pa} and b_i with increase in iteration number is shown in Fig. 3.

$$C_i = \ln\left(\frac{b_i^L}{b_i^U}\right) \quad (8)$$

$$b_i(k) = b_i^U * \exp(C_i * k) \quad (9)$$

$$R_{pa}(k) = R_{pa}^L + \frac{(R_{pa}^U - R_{pa}^L)}{k_{max}} * k \quad (10)$$

where b_i^U and b_i^L are the lower and upper bounds of the distance bandwidth respectively, R_{pa}^U and R_{pa}^L are the upper and lower bounds of the pitch adjusting rates respectively, k_{max} is the maximum number of iterations, k and is the current iteration.

Step 4: Update the new harmony

If the new solution vector is better than the worst one in the HM judged in terms of objective function value, the worst one will be replaced by the new one in the HM.

Table 8
Tuned parameters of coordinated damping controllers using GA, PSO, HSA and BSO.

Location	Controller	Coordinated design using GA			Coordinated design using PSO			Coordinated design using HSA			Coordinated design using BSO		
		K	T_1	T_2	K	T_1	T_2	K	T_1	T_2	K	T_1	T_2
G1	PSS	31.9574	0.6310	0.1497	39.7880	0.3987	0.1002	8.4667	0.6067	0.1133	26.2845	0.6425	0.0428
G2	PSS	28.7563	0.8701	0.3906	40.7571	0.5737	0.2498	14.0667	0.6427	0.1133	12.8566	0.6875	0.1893
G3	PSS	22.7592	0.6425	0.0773	38.0179	0.4186	0.1535	14.0667	0.6267	0.2333	11.5556	0.6832	0.1882
G4	PSS	1.6534	0.9064	0.1895	2.3953	0.4098	0.0472	12.2000	0.6600	0.2067	4.4392	0.6022	0.1996
G5	PSS	18.1713	0.5660	0.4651	10.7520	0.3448	0.2099	10.3333	0.5533	0.2067	20.1588	0.5978	0.1254
G6	PSS	13.3569	0.9110	0.2405	46.4748	0.3338	0.1094	6.6000	0.7133	0.2067	26.9422	0.8304	0.1688
G7	PSS	34.5109	0.6086	0.4676	20.6541	0.1998	0.1559	6.6000	0.8733	0.1400	10.9898	0.6767	0.1012
G8	PSS	5.0671	0.6626	0.4008	26.0415	0.4246	0.2005	2.8667	0.6600	0.2200	8.7575	0.8455	0.0345
G9	PSS	7.8578	0.9483	0.1722	29.8426	0.3096	0.1297	8.4667	0.6333	0.2200	5.6288	0.8412	0.1869
G10	PSS	21.7755	0.6953	0.3175	29.9455	0.4498	0.1005	8.4667	0.6867	0.3000	44.2864	0.9825	0.2124
26-29	TCSC	27.85	0.5692	0.3224	45.92	0.7438	0.3897	45.2785	0.5845	0.3292	32.26	0.6132	0.2826

Table 9
Comparison of eigenvalues and damping ratios using GA, PSO, HSA, BSO and IHSA based coordinated damping controllers.

	GAPSS + GATCSC	**PSOPSS + PSOTCSC**	**HSAPSS + HSATCSC**	**BSOPSS + BSOTCSC**	**IHSAPSS + IHSATCSC**
Scenario 1	−0.6917 ± 12.6077i, 0.0548	−4.8532 ± 11.8028i, 0.3803	−1.6203 ± 11.5720i, 0.1387	−2.3285 ± 11.1402i, 0.2046	−2.3661 ± 11.4315i, 0.2027
	−0.6282 ± 10.3659i, 0.0605	−1.4598 ± 13.3108i, 0.1090	−3.6322 ± 7.4414i, 0.4386	−1.6689 ± 11.2509i, **0.1467**	−2.0343 ± 10.6661i, **0.1874**
	−**0.3535** ± **10.4114i, 0.0339**	−1.9942 ± 12.7197i, 0.1549	−**0.9956** ± **9.5492i, 0.1037**	−3.3852 ± 9.6463i, 0.3311	−2.3746 ± 8.9921i, 0.2553
	−0.6843 ± 9.3642i, 0.0729	−**0.6765** ± **11.6848i, 0.0578**	−1.2463 ± 9.7595i, 0.1267	−1.9386 ± 10.0298i, 0.1898	−**1.9439** ± **8.7168i,** 0.2177
	−1.5065 ± 8.8559i, 0.1677	−0.9737 ± 9.3240i, 0.1039	−1.3422 ± 9.2087i, 0.1442	−1.5313 ± 9.8321i, 0.1539	−3.7288 ± 6.0353i, 0.5256
	−0.8057 ± 6.7671i, 0.1182	−1.2737 ± 7.9850i, 0.1575	−1.4762 ± 8.0834i, 0.1796	−2.8266 ± 5.1077i, 0.4842	−2.9649 ± 4.5378i, 0.5470
	−2.6875 ± 3.6331i, 0.5947	−1.2638 ± 6.1960i, 0.1999	−2.6379 ± 3.8387i, 0.5664	−2.0861 ± 3.5333i, 0.5084	−2.1137 ± 3.6619i, 0.4999
	−1.7647 ± 3.5259i, 0.4476	−1.1928 ± 3.1623i, 0.3529	−2.3177 ± 3.3553i, 0.5683	−1.3185 ± 2.2638i, 0.5033	−2.5393 ± 3.4123i, 0.5970
	−1.2692 ± 3.3035i, 0.3586	−1.7415 ± 2.4798i, 0.5747	−1.0082 ± 3.3669i, 0.2869	−**1.1487** ± **1.9274i,** 0.5120	−2.0725 ± 3.3061i, 0.5311
Scenario 2	−0.5865 ± 12.3722i, 0.0474	−4.8734 ± 11.7816i, 0.3822	−1.6122 ± 11.5417i, 0.1383	−2.3405 ± 11.1349i, 0.2057	−2.0493 ± 10.6651i, **0.1887**
	−**0.3850** ± **10.4012i, 0.0370**	−1.9831 ± 12.6903i, 0.1544	−1.0295 ± 9.5749i, **0.1069**	−1.6689 ± 11.2254i, **0.1471**	−3.5043 ± 9.8431i, 0.3354
	−0.8927 ± 9.8812i, 0.0900	−**0.6899** ± **11.6846i, 0.0589**	−1.2658 ± 9.6293i, 0.1303	−3.4003 ± 9.6539i, 0.3322	−2.2356 ± 9.7855i, 0.2227
	−0.7125 ± 9.1170i, 0.0779	−1.2828 ± 8.8452i, 0.1435	−3.6593 ± 7.4204i, 0.4423	−1.9434 ± 9.9961i, 0.1908	−**1.7076** ± **8.3194i,** 0.2011
	−1.5979 ± 8.6491i, 0.1817	−1.3547 ± 7.9549i, 0.1679	−1.6236 ± 8.2926i, 0.1921	−1.5289 ± 9.8135i, 0.1539	−3.6894 ± 6.0566i, 0.5202
	−0.7651 ± 6.7958i, 0.1119	−1.1571 ± 6.2555i, 0.1819	−1.4576 ± 8.0547i, 0.1781	−2.7987 ± 5.0777i, 0.4827	−2.6117 ± 4.3178i, 0.5176
	−2.7483 ± 3.6108i, 0.6057	−1.1625 ± 3.0949i, 0.3516	−2.3875 ± 3.8576i, 0.5263	−2.0324 ± 3.4491i, 0.5077	−2.9883 ± 3.5750i, 0.6413
	−1.7844 ± 3.5101i, 0.4532	−1.4811 ± 2.4881i, 0.5115	−**0.9775** ± **3.3503i,** 0.2801	−1.3080 ± 2.2638i, 0.5003	−1.8910 ± 3.7298i, 0.4522
	−1.2582 ± 3.3098i, 0.3553	−2.4224 ± 2.1312i, 0.7508	−2.3426 ± 3.3228i, 0.5762	−**1.1594** ± **1.9260i,** 0.5157	−1.9519 ± 3.2304i, 0.5171
Scenario 3	−0.6360 ± 12.2578i, 0.0518	−4.9889 ± 11.7527i, 0.3907	−1.5908 ± 11.5063i, 0.1369	−2.3441 ± 11.1132i, 0.2064	−2.6235 ± 12.6693i, 0.2028
	−**0.3810** ± **10.4071i, 0.0366**	−1.5457 ± 13.2553i, 0.1158	1.0496 ± 9.5498i, **0.1092**	−1.6595 ± 11.2000i, **0.1466**	−3.7998 ± 10.1122i, 0.3518
	−0.8428 ± 9.7069i, 0.0865	−2.0084 ± 12.6366i, 0.1570	−1.2644 ± 9.5698i, 0.1310	−3.4105 ± 9.6429i, 0.3334	−2.0342 ± 10.6655i, **0.1874**
	−1.7062 ± 8.7588i, 0.1912	−**0.6841** ± **11.6994i, 0.0584**	−3.7184 ± 7.5509i, 0.4418	−1.9386 ± 9.9965i, 0.1904	−1.8456 ± 9.6184i, 0.1884
	−0.6920 ± 8.9882i, 0.0768	−1.2287 ± 8.6903i, 0.1400	−1.6210 ± 8.2335i, 0.1932	−1.5210 ± 9.6288i, 0.1560	−**1.8292** ± **8.0582i,** 0.2214
	−0.7963 ± 6.7567i, 0.1170	−1.2983 ± 7.9971i, 0.1602	−1.4918 ± 8.0331i, 0.1826	−2.7900 ± 5.0750i, 0.4818	−3.6881 ± 6.0703i, 0.5192
	−2.7473 ± 3.6285i, 0.6036	−1.1596 ± 6.1662i, 0.1848	−2.3880 ± 3.8832i, 0.5238	−2.0127 ± 3.4595i, 0.5029	−2.5788 ± 4.3477i, 0.5102
	−1.7755 ± 3.5088i, 0.4515	−1.1415 ± 3.0901i, 0.3465	−2.3313 ± 3.3643i, 0.5696	−1.2911 ± 2.2916i, 0.4909	−1.8696 ± 3.7245i, 0.4486
	−1.2371 ± 3.3201i, 0.3492	−1.4683 ± 2.4851i, 0.5087	−**0.9268** ± **3.3041i,** 0.2701	−**1.1791** ± **1.9282i,** 0.5217	−1.9653 ± 3.2309i, 0.5197
Scenario 4	−0.5953 ± 12.3048i, 0.0483	−5.0340 ± 11.7321i, 0.3943	−1.5925 ± 11.4887i, 0.1373	−2.3432 ± 11.1040i, 0.2065	−2.7947 ± 12.7309i, 0.2144
	−**0.3729** ± **10.4246i, 0.0358**	−1.5578 ± 13.2096i, 0.1171	−1.0509 ± 9.5385i, **0.1095**	−1.6481 ± 11.1885i, **0.1457**	−3.7330 ± 10.3166i, 0.3403
	−0.8016 ± 9.6514i, 0.0828	−2.0517 ± 12.5967i, 0.1608	−1.2757 ± 9.5254i, 0.1327	−3.4226 ± 9.6344i, 0.3348	−2.0218 ± 10.6883i, 0.1859
	−1.8413 ± 8.9190i, 0.2022	−**0.6783** ± **11.7277i, 0.0577**	−3.6765 ± 7.7399i, 0.4291	−1.9439 ± 9.9893i, 0.1910	−**1.7136** ± **9.6083i, 0.1756**
	−0.6553 ± 8.9625i, 0.0729	−1.2247 ± 8.7873i, 0.1380	−1.6222 ± 8.1542i, 0.1951	−1.4955 ± 9.5597i, 0.1546	−1.7885 ± 7.9247i, 0.2202
	−0.7609 ± 6.7577i, 0.1119	−1.2880 ± 8.0739i, 0.1575	−1.5087 ± 8.0118i, 0.1851	−2.7877 ± 5.0874i, 0.4805	−3.6869 ± 6.0807i, 0.5185
	−2.7620 ± 3.6064i, 0.6080	−1.1051 ± 6.1810i, 0.1760	−2.3242 ± 3.8732i, 0.5145	−1.6861 ± 2.9003i, 0.5026	−2.5093 ± 4.3073i, 0.5034
	−1.7828 ± 3.4965i, 0.4542	−1.1167 ± 3.0576i, 0.3431	−2.3300 ± 3.3726i, 0.5684	−1.2812 ± ± 2.3054i, 0.4858	−1.7991 ± 3.7173i, 0.4356
	−1.2218 ± 3.3197i, 0.3454	−1.4048 ± 2.5248i, 0.4862	−**0.8978** ± **3.2613i,** 0.2654	−**1.1998** ± **1.9316i,** 0.5277	−1.9405 ± 3.2146i, 0.5168

Step 5: Check for the termination condition

The IHSA will be terminated when the termination condition is met. This may be usually a sufficiently good objective function value or a maximum number of iterations. The maximum number of iterations criterion is employed in this work. The flowchart IHSA is shown in Fig. 4.

4. Simulation results

The algorithm was developed in MATLAB and simulations were carried out on a computer with Intel Core i3 CPU, 2.27 GHz and 4 GB RAM.

Test System 1: WSCC 3-machine, 9-bus system

The proposed IHSA is applied on WSCC 3-machine, 9-bus system shown in Fig. 5. Power flow, transmission line and dynamic data for the generators can be found in [43], and all generators are represented by fifth order model. Here it is assumed that generators are equipped with PSS. For illustration and comparison purpose of an 'n' generator system, the (n–1) electromechanical modes associated with generator rotors are considered. The power flow in line 5–7 is the largest and therefore this line is considered as the best location for installing the TCSC controller in the system under study.

The system generations and loading levels considered in this study are given in Table 1. The tuned parameters of PSS and TCSC obtained by BSO and IHSA algorithms are given in Table 2 and 3 shows comparison of eigenvalues and damping ratios of electro-mechanical mode of oscillations using BSO and IHSA based coordinated damping controllers at different loading levels. In all the three loading levels, IHSA based damping controllers are giving better damping factors and better damping ratio compared to BSO based controllers. The corresponding values of damping ratios and damping factors are highlighted in Table 3. IHSA based coordinated controllers shifts the electromechanical mode eigenvalues are further to the left half of *s*-plane and damping ratios are obtained also greater than that of BSO based damping controllers for all the loading conditions.

Table 10
Different contingencies considered for non-linear time domain simulations.

Contingency	Description
Contingency (a)	A six-cycle three-phase fault, very close to the 14th bus in the line 4–14, which is cleared by tripping the line 4–14.
Contingency (b)	A six-cycle fault disturbance at bus 33 at the end of line 19–33 with the load at bus-25 doubled and is cleared by tripping the line 19–33 with successful reclosure after 1.0 s.
Contingency (c)	A critical six cycle three-phase fault close to 22nd bus in the line 22–35 with load at 21st bus increased by 20% & load at 25th bus and is cleared by tripping the line 22–35 with successful reclosure after 1.0 s.
Contingency (d)	A six-cycle three-phase fault, near bus 14 in the line 14–15 with 20% increase in load, which is cleared by tripping the line 14–15.

Test System 2: New England 10-machine, 39-bus system

The proposed technique is applied on New England 10-machine, 39-bus system shown in Fig. 6, for which power flow, transmission line and dynamic data for the generators can be found in [44]. All generators are represented by fifth order model, and are assumed to be equipped with PSS. To find the optimum location for TCSC, different locations are tested by residue method [45]. Residues associated with critical mode are calculated using the transfer function between the TCSC active power deviation ΔP and degree of compensation ΔK_c (in p.u. of line reactance) are shown in Table 4. Line

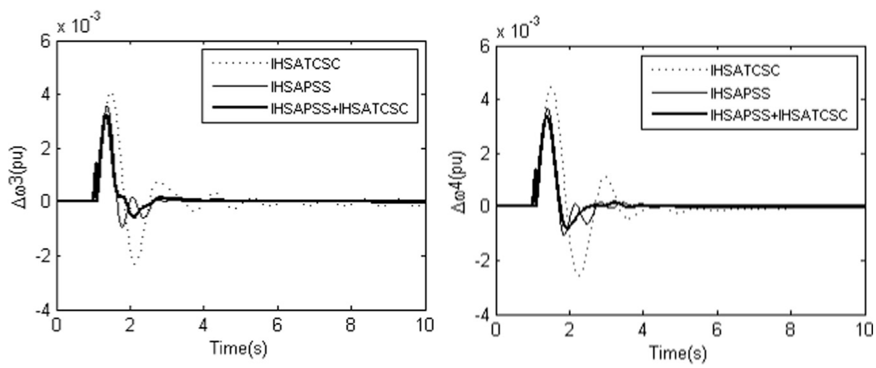

Fig. 7. Speed deviations of 3rd and 4th generators for Contingency (a).

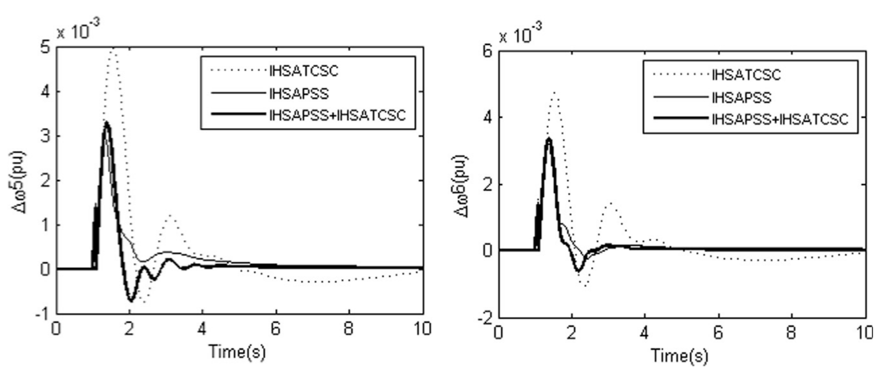

Fig. 8. Speed deviations of 5th and 6th generators for Contingency (b).

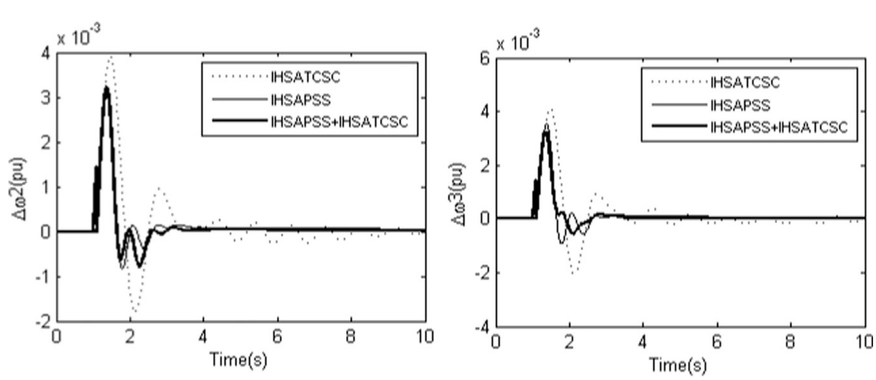

Fig. 9. Speed deviations of 2nd and 3rd generators for Contingency (c).

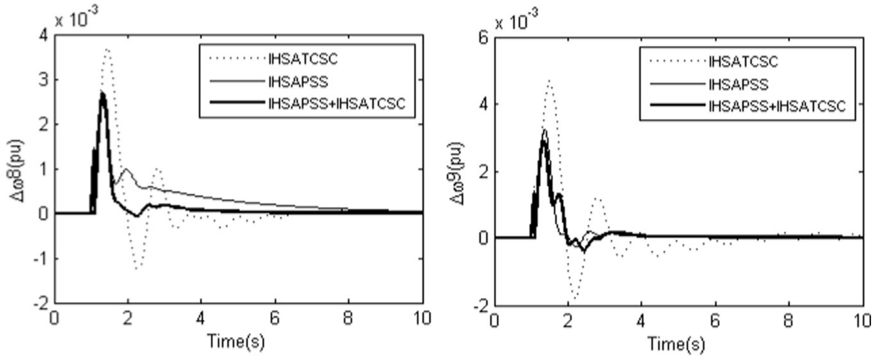

Fig. 10. Speed deviations of 8th and 9th generators for Contingency (d).

Table 11
Values of performance index for IHSATCSC, IHSAPSS and coordinated IHSAPSS & IHSATCSC.

	IHSATCSC	IHSAPSS	IHSAPSS+IHSATCSC
Contingency (a)	10.6611	3.0916	3.0588
Contingency (b)	10.7682	3.5103	3.4836
Contingency (c)	10.5717	3.6345	3.6085
Contingency (d)	9.2405	3.4698	3.4551

26–29 has largest residue value and is therefore most effective location for placement of TCSC.

4.1. Eigenvalue analysis

To assess the effectiveness and robustness of the proposed IHSA based coordinated damping controllers, four different operating scenarios that represent the system under severe loading conditions and critical line outages are considered. These conditions are extremely hard from the stability point of view [46]. The different operating scenarios considered are given in Table 5. The tuned parameters of PSS and TCSC both for uncoordinated and coordinated design using proposed IHSA are shown in Table 6.

The electromechanical modes and the damping ratios obtained for all the above cases without controller, independently designed IHSA based TCSC (IHSATCSC), IHSA based PSS (IHSAPSS) and coordinated PSS and TCSC are given in Table 7.

The critical eigenvalues and damping ratios are highlighted in Table 7. From Table 7, it is clear that the system with IHSATCSC is suffered from small damping factor ($\sigma = -0.1037$, -0.1528, -0.0980 and -0.0933) for all these operating scenarios. Further the proposed coordinated controllers shift substantially the electromechanical mode eigenvalues to the left of s-plane and the values of the damping factors with the proposed coordinated controllers are significantly improved ($\sigma = -1.9439$, -1.7076, -1.8292 and -1.7136). The damping ratios corresponding to coordinated controllers ($\zeta = 18.74\%$, 18.87%, 18.74% and 17.56%) are much better than corresponding IHSATCSC values ($\zeta = 1.62\%$, 2.20%, 1.53% and 1.46%). Hence compared to the uncoordinated IHSATCSC and IHSAPSS, the proposed coordinated controllers greatly enhance the system stability and improve the damping characteristics of electromechanical modes of oscillations.

The tuned parameters of PSS and TCSC both for coordinated design using GA, PSO, HSA, BSO and IHSA are shown in Table 8. To demonstrate the effectiveness of the proposed technique, the electromechanical modes and the damping ratios obtained for all the above cases are compared with GA, PSO, HSA and BSO based coordinated damping controllers are given in Table 9.

It is evident from Table 9 that with the proposed IHSA based coordinated controllers, poorly damped electromechanical mode eigenvalues are further shifted to the left of s-plane for all the operating scenarios. Further, the damping ratios of critical electromechanical modes are also significantly enhanced with the proposed IHSA based coordinated PSS and TCSC.

The various parameters of GA, PSO, BSO and IHSA optimization techniques are given in Appendix. The computational time for IHSA is 284.6 s while it is 356.6 s, 366.8 s and 492.4 s for GA, PSO and BSO respectively. It was found that the IHSA converges at a faster rate in less number of iterations and achieves a better minimum fitness value for the objective function as compared to GA, PSO and BSO.

4.2. Nonlinear time domain simulations

To investigate the robustness of the coordinated design of PSS and TCSC using Improved Harmony Search Algorithm over a wide range of operating conditions and system configurations, nonlinear time domain simulation studies are carried out for the contingencies shown in Table 10 on the system under study. System performance is demonstrated by using the performance index, Integral of Time multiplied Absolute value of Error (*ITAE*), given by $PI = ITAE = \int_0^n t.(|\Delta\omega_1| + |\Delta\omega_2| + \ldots + |\Delta\omega_n|)$ (8), where 'n' is the number of generators of that system. It is worth mentioning that the lower the value of this index is, better the system response in terms of time domain characteristics.

The speed deviations of critical generators for these contingencies with uncoordinated IHSATCSC, IHSAPSS and with the proposed coordinated IHSA based PSS and TCSC are shown in Figs. 7–10 respectively. These figures validate the superiority of the proposed method in tuning coordinated controllers for damping system oscillations.

The performance index (*ITAE*) obtained for the above contingencies using these controllers are given in Table 11.

It is clear from the simulation studies that simultaneous coordinated design of the PSS and TCSC damping controllers show better damping performance over uncoordinated damping controllers under different disturbances.

The performance index (*ITAE*) obtained for the above contingencies using GA, PSO, BSO and IHSA based coordinated damping controllers are given in Table 12.

It is also clear from the above table that performance indices for IHSA based coordinated damping controllers are less than the corresponding values of GA, PSO, HSA and BSO based coordinated damping controllers, which demonstrate the superior performance

Table 12
Performance index values.

	GAPSS + GATCSC	PSOPSS + PSOTCSC	HSAPSS + HSATCSC	BSOPSS + BSOTCSC	IHSAPSS + IHSATCSC
Contingency (a)	6.9713	6.6408	5.9140	5.8846	3.0588
Contingency (b)	7.0013	6.6811	5.7403	5.8078	3.4836
Contingency (c)	6.8893	6.5832	5.7558	5.8019	3.6085
Contingency (d)	7.0203	6.5452	5.6159	5.1858	3.4551

of these controllers in enhancing the system stability and in improving the damping characteristics of electromechanical modes.

5. Conclusions

This paper presents a robust design algorithm for simultaneous coordinated tuning of PSS and TCSC damping controllers in a multi-machine power system. The problem of tuning the PSS and TCSC damping controller parameters simultaneously, in order to enhance the damping of the power oscillations is formulated as a multi-objective optimization problem and IHSA has been successfully applied to search for optimal controllers parameters. The damping ratio and damping factors of electromechanical modes of oscillations obtained by using IHSA on WSCC 3-machine, 9-bus system are found be superior compared to the results obtained using Bacterial Swarm Optimization (BSO) and other algorithms. The damping performance of PSS and TCSC controllers when they are designed independently using IHSA is compared with coordinated design of IHSA based PSS and TCSC on New England 10-machine, 39-bus system at different operating scenarios and contingencies. The eigenvalue analysis and nonlinear simulation results demonstrate the effectiveness and robustness of the proposed IHSA based coordinated controllers over the Genetic Algorithm (GA), Particle Swarm Optimization (PSO), Harmony Search Algorithm (HSA) and Bacterial Swarm Optimization (BSO) based coordinated damping controllers.

Appendix

Parameters of Genetic Algorithm	
Termination parameter, ε	:0.0001
Crossover probability, p_c	:0.8
Mutation probability, p_m	:0.05
Maximum number of iterations, $t_{\max}$	:100
Parameters of Particle Swarm Optimization	
Positive constants	:$C_1 = 2.4$, $C_2 = 1.6$
Number of particles	:25
Maximum number of iterations, $t_{\max}$	:100
Parameters of Harmony Search Algorithm	
Maximum number of iterations	= 50
Memory size (HMS)	= 20
Harmony memory considering rate (HMCR)	= 0.6
Pitch Adjusting Rate	= 0.3
Band width	= 0.001
Parameters of Bacterial Swarm Optimization	
Number of dimensions of search space	= 20
Number of bacteria	= 6
Number of chemotactic steps	= 6
Number of elimination and dispersal events	= 2
Number of reproduction steps	= 50
Probability of elimination and dispersal	= 0.25
Parameters of Improved Harmony Search Algorithm	
Maximum number of iterations	= 0
Memory size (HMS)	= 20
Harmony memory considering rate (HMCR)	= 0.6
Pitch adjusting rate bounds $R^U_{pa} = 0.9$ and $R^L_{pa} = 0.1$	
Band width bounds $b^U_i = 1.0$ and $b^L_i = 0.0001$	

References

[1] Y.N. Yu, Electric Power System Dynamics, Academic Press, New York, 1983.
[2] P. Kundur, M. Klein, G.J. Rogers, M.S. Zywno, Application of power system stabilizers for enhancement of overall system stability, IEEE Trans. Power Syst. 4 (2) (1989) 614–626.
[3] Y.L. Abdel-Magid, M.A. Abido, S. Al-Baiyat, A.H. Mantawy, Simultaneous stabilization of multi-machine stabilizers via genetic algorithm, IEEE Trans. Power Syst. 14 (4) (1999) 1428–1439.

[4] Y.L. Abdel-Magid, M.A. Abido, Optimal multi-objective design of robust power system stabilizers using genetic algorithms, IEEE Trans. Power Syst. 18 (3) (2003) 1125–1132.
[5] M.A. Abido, Y.L. Abdel-Magid, Eigenvalue assignments in multi-machine power systems using tabu search algorithm, Comput. Electr. Eng. 28 (2002) 527–545.
[6] M.A. Abido, Robust design of multi-machine power system stabilizers using simulated annealing, IEEE Trans. Energy Convers. 15 (3) (2000) 297–304.
[7] M.A. Abido, Optimal design of power system stabilizers using particle swarm optimization, IEEE Trans. Energy Convers. 17 (3) (2002) 406–413.
[8] C. Ardil Sidhartha Panda, Robust coordinated design of multiple power system stabilizers using particle swarm optimization technique, Int. J. Electr. Electron. Eng. 1 (1) (2008) 1–8.
[9] G. Naresh, M. Ramalinga Raju, S.V.L. Narasimham, K. Ravindra, Tuning of power system stabilizers in multi-machine systems using particle swarm optimization, Int. Rev. Model. Simul. 4 (5) (2011) 2470–2479.
[10] S. Mishra, M. Tripathy, J. Nanda, Multi-machine power system stabilizer design by rule based bacterial foraging, Electr. Power Syst. Res. 77 (2007) 1595–1607.
[11] G. Naresh, M. Ramalinga Raju, S.V.L. Narasimham, Application of harmony search algorithm for the robust design of power system stabilizers in multi-machine power systems, J. Electr. Eng. Rom. 13 (2013) 9–19 (Edition 2, Article 13.2.2).
[12] L. Gyugyi, N.G. Hingorani, Understanding FACTS: Concepts and Technology of Flexible AC Transmission Systems, Wiley John & Sons, Incorporated, New York, 1999.
[13] N. Yang, Q. Liu, J.D. McCalley, TCSC controller design for damping inter-area oscillations, IEEE Trans. Power Syst. 13 (4) (1998) 1304–1310.
[14] B.H. Li, Q.H. Wu, D.R. Turner, P.Y. Wang, X. Zhou, Modeling of TCSC dynamics for control and analysis of power system stability, Int. J. Electr. Power Energy Syst. 22 (1) (2000) 43–49.
[15] L. Fan, A. Feliachi, K. Schoder, Selection and design of a TCSC control signal in damping power system inter-area oscillations for multiple operating conditions, Int. J. Electr. Power Energy Syst. 62 (2) (2002) 127–137.
[16] A.D. Del Rosso, C.A. Canizares, V.M. Dona, A study of TCSC controller design for power system stability improvement, IEEE Trans. Power Syst. 18 (4) (2003) 1487–1496.
[17] S. Hameed, B. Das, V. Pant, Reduced rule base self tuning fuzzy PI controller for TCSC, Int. J. Electr. Power Energy Syst. 32 (9) (2010) 1005–1013.
[18] L. Khan, I. Ullah, T. Saeed, K.L. Lo, Virtual Bees algorithm based design of damping control system for TCSC, Aust. J. Basic Appl. Sci. 4 (1) (2010) 1–18.
[19] E.S. Ali, S.M. Abd-Elazim, TCSC damping controller design based on bacteria foraging optimization algorithm for a multi-machine power system, Int. J. Electr. Power Energy Syst. 37 (2012) 23–30.
[20] Y. Wang, David J. Hill, Robust nonlinear coordinated control of power systems, Automatica 32 (4) (1996) 611–618.
[21] Gilles Trudel Innocent Kamwa, Luc G.érin Lajoie, Robust design and coordination of multiple damping controllers using nonlinear constrained optimization, IEEE Trans. Power Syst. 15 (3) (2000) 1084–1092.
[22] Rodrigo A. Ramos, Luis F.C. Alberto, Newton G. Bretas, A new methodology for the coordinated design of robust decentralized power system damping controllers, IEEE Trans. Power Syst. 19 (1) (2004) 444–454.
[23] X. Lei, E.N. Lerch, D. Povh, Optimization and coordination of damping controls for improving system dynamic performance, IEEE Trans. Power Syst. 16 (3) (2001) 473–480.
[24] L.J. Cai, I. Erlich, Simultaneous coordinated tuning of PSS and FACTS controller for damping power system oscillations in multi-Machine systems, in: Proceedings of IEEE Bologna Power Tech Conference, 2003, pp. 1–6.
[25] R. You, M.H. Nehrir, D.A. Pierre, Controller design for SVC and TCSC to enhance damping of power system oscillations, Int. J. Electr. Power Compon. Syst. 35 (2007) 871–884.
[26] M.A. Abido, Y.L. Abdel Majid, Coordinated design of a PSS and an SVC-based controller to enhance power system stability, Int. J. Electr. Power Energy Syst. 25 (2003) 695–704.
[27] H. Shayeghi, A. Safari, H.A. Shayanfar, PSS and TCSC damping controller coordinated design using PSO in multi-machine power system, Int. J. Energy Convers. Manag. 51 (12) (2010) 2930–2937.
[28] D.B. Fogel, Evolutionary computation towards a new philosophy of machine intelligence, IEEE Press, New York, 1995.
[29] D.P. Rini, S.M. Shamsuddin, S.S. Yuhaniz, Particle swarm optimization: technique, system and challenges, Int. J. Comput. Appl. 14 (1) (2011) 19–27.
[30] M. Gitizadeh, S. Ghavidel, Improving transient stability with multi-objective allocation and parameter setting of SVC in a multi-machine power system, IETE J. Res. 60 (1) (2014) 33–41.
[31] B. Bahmani-Firouzi, E. Farjah, R. Azizipanah-Abarghooee, An efficient scenario-based and fuzzy self-adaptive learning particle swarm optimization approach for dynamic economic emission dispatch considering load and wind power uncertainties, Energy 50 (2013) 232–244.
[32] E.S. Ali, S.M. Abd-Elazim, Coordinated design of PSSs and TCSC via bacterial swarm optimization algorithm in a multi-machine power system, Int. J. Electr. Power Energy Syst. 36 (1) (2012) 84–92.
[33] Xin-She Yang, Seyyed Soheil Sadat Hosseini, Amir Hossein Gandomi, Firefly Algorithm for solving non-convex economic dispatch problems with valve loading effect, Appl. Soft Comput. 12 (2012) 1180–1186.
[34] R. Azizipanah-Abarghooee, A new hybrid bacterial foraging and simplified swarm optimization algorithm for practical optimal dynamic load dispatch, Int. J. Electr. Power Energy Syst. 49 (2013) 414–429.
[35] M. Ghasemi, M.M. Ghanbarian, S. Ghavidel, S. Rahmani, E. Mahboubi-Moghaddam, Modified teaching learning algorithm and double differential evolution algorithm for optimal reactive power dispatch problem: a comparative study, Inf. Sci. 278 (2014) 231–249.
[36] M. Ghasemi, S. Ghavidel, M.M. Ghanbarian, A. Habibi, A new hybrid algorithm for optimal reactive power dispatch problem with discrete and continuous control variables, Appl. Soft Comput. 22 (2014) 126–140.
[37] M. Ghasemi, S. Ghavidel, M.M. Ghanbarian, H.R. Massrur, M. Gharibzadeh., Application of imperialist competitive algorithm with its modified techniques for multi-objective optimal power flow problem: a comparative study, Inf. Sci. 281 (2014) 225–247.
[38] M. Ghasemi, S. Ghavidel, S. Rahmani, A. Roosta, H. Falah, A novel hybrid algorithm of imperialist competitive algorithm and teaching learning algorithm for optimal power flow problem with non-smooth cost functions, Eng. Appl. Artif. Intell. 29 (2014) 54–69.
[39] M. Ishimaru, R. Yokoyama, G. Shirai, T. Niimura, Robust thyristor controlled series capacitor controller design based on linear matrix inequality for a multi-machine power system, Int. J. Electr. Power Energy Syst. 24 (8) (2002) 621–629.
[40] Z.W. Geem, Novel derivative of harmony search algorithm for discrete design variables, Appl. Math. Comput. 199 (1) (2008) 223–230.
[41] Zong Woo Geem, Recent Advances in Harmony Search Algorithm, Springer-Verlag, Berlin, Heidelberg, 2010.
[42] M. Mahdavi, M. Fesanghary, E. Damangir, An improved harmony search algorithm for solving optimization problems, Appl. Math. Comput. 188 (2007) 1567–1579.
[43] P.W. Sauer, M.A. Pai, Power System Dynamics and Stability, Prentice-Hall, Englewood Cliffs, NJ, 1998.
[44] M.A. Pai, Energy Function Analysis for Power System Stability, Kluwer, Norwell, MA, 1989.
[45] R. Sadikovic, Use of FACTS Devices for Power Flow Control and Damping of Oscillations in Power Systems (Dissertation), Swiss Federal Institute of Technology, Zurich, 2006.
[46] A. Bazanella, A. Fischman, A. Silva, J. Dion, L. Dugrad, Coordinated robust controllers in power systems, in: Proceedings of IEEE Stockholm Power Tech Conference, 1995, pp. 256–261.